

Supporting information

S1 File. GISAID Acknowledge table

S2 File GISAID accession IDs and metadata of the sequences used for constructing genealogy

S3 File GISAID accession IDs and metadata of the sequences used in the analysis of subclade frequency

Supplementary Figures

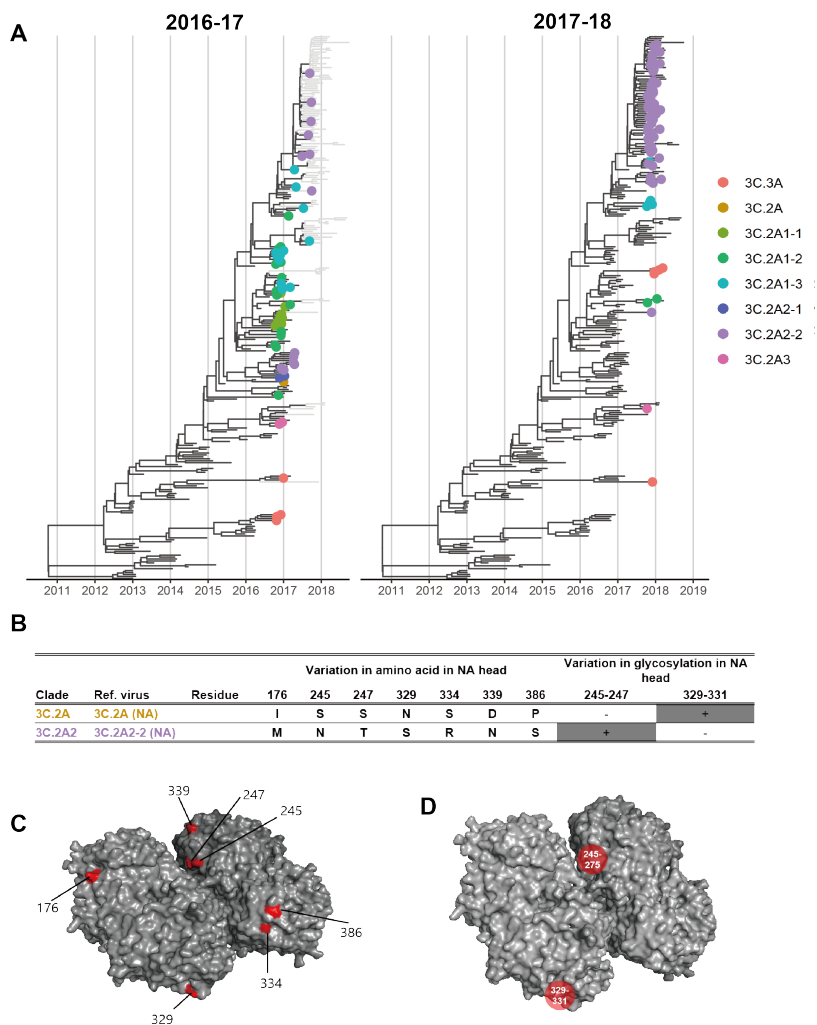


Fig S1. NA of co-circulating H3N2 clades during the 2016-17 and 2017-18 seasons. A. Genealogy of H3N2 showing NA sequence samples through the 2016-17 season (left) and through the 2017-18 season (right). Tips are filled circles if collected in North America during the 2016-17 season (left) and the 2017-18 season (right) and colored according to the associated test virus. B. Variable amino acids and PNGS between test viruses. Between clade 3C.2A (NA) and clade 3C.2A2 (NA), only substitutions at NA head are shown. C. The differences between clade 3C.2A (NA) and 3C.2A2-2 (NA) are shown on N2 head structure (Protein Data Bank: 6n4d). Amino acid differences between the two test viruses are colored in red. D. PNGS that vary between 3C.2A (NA) and 3C.2A2 (NA) are shown on the N2 structure.

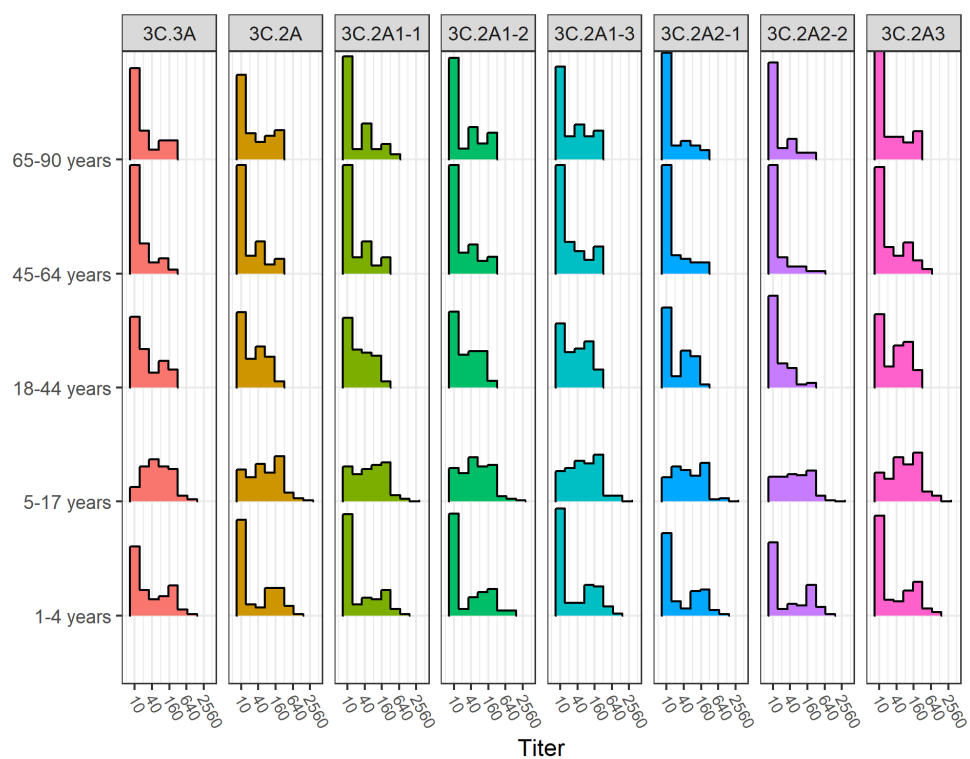


Fig S2. Distribution of HA titers for each strain by age group. A titer of 10 indicates the titer is below the limit of detection.

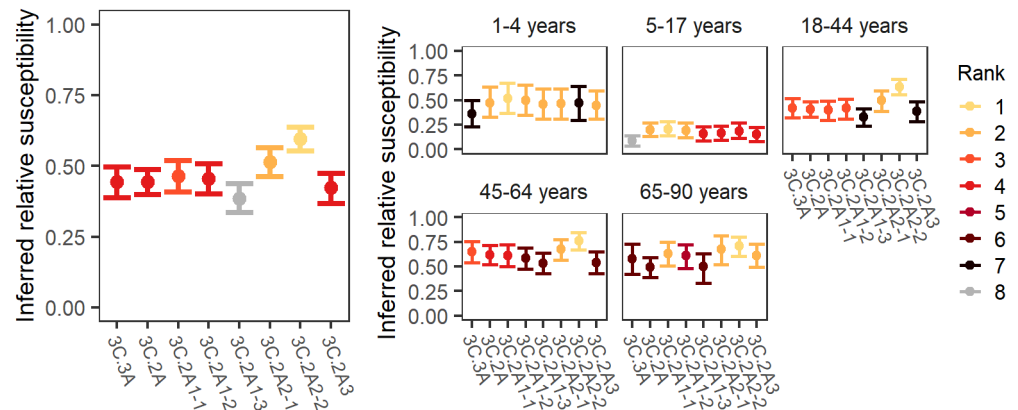


Fig S5. The inferred relative susceptibility and its rank to each HA reference strain using a 1:20 titer threshold. Inferred relative susceptibility and its rank to each reference strain for the whole population (left) and by age group (right). The bars indicate 95% CIs obtained from bootstrapping. Lower ranks (closer to 1) indicate greater susceptibility.

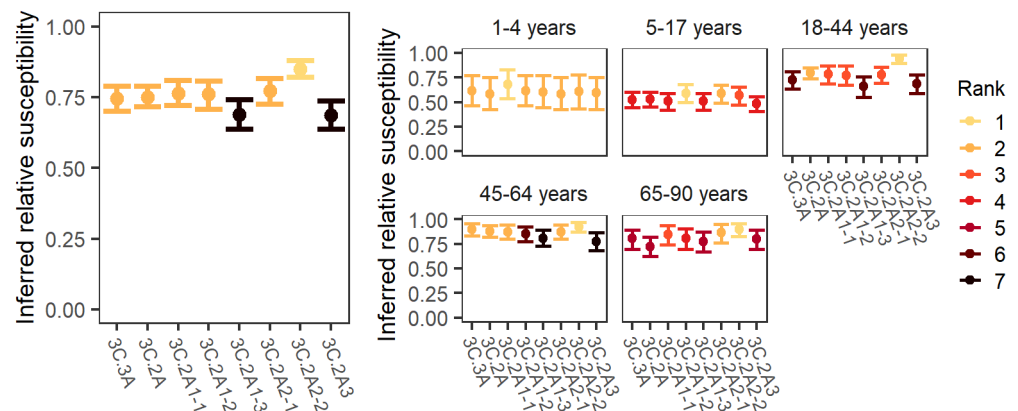


Fig S6. The inferred relative susceptibility and its rank to each HA reference strain using a 1:80 titer threshold. Inferred relative susceptibility and its rank to each reference strain for the whole population (left) and by age group (right). The bars indicate 95% CIs obtained from bootstrapping. Lower ranks (closer to 1) indicate greater susceptibility.

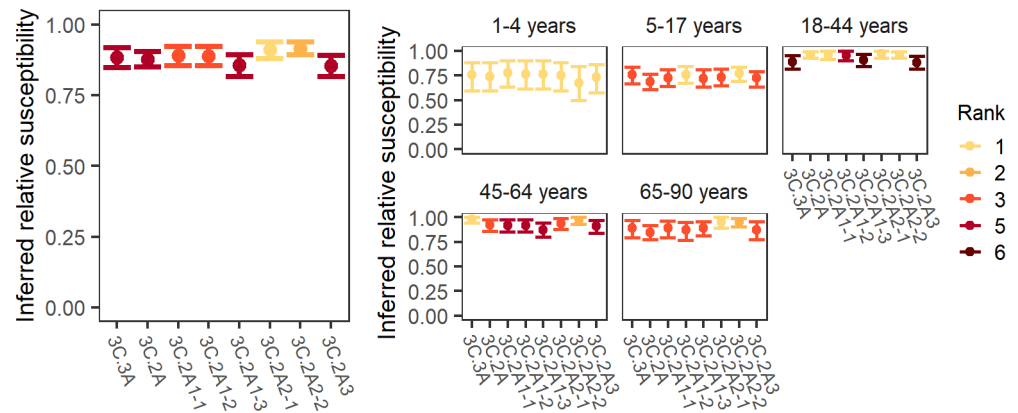


Fig S7. The inferred relative susceptibility and its rank to each HA reference strain using a 1:160 titer threshold. Inferred relative susceptibility and its rank to each reference strain for the whole population (left) and by age group (right). The bars indicate 95% CIs obtained from bootstrapping. Lower ranks (closer to 1) indicate greater susceptibility.

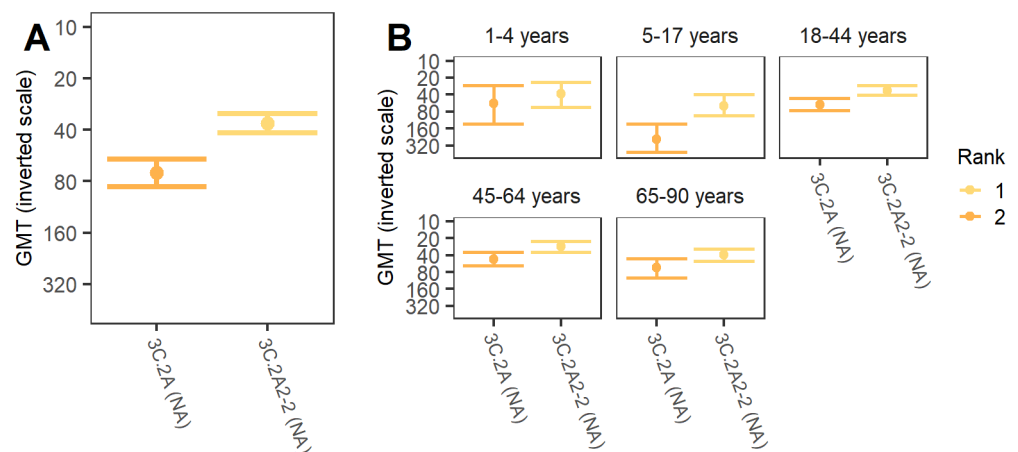


Fig S8. The relative susceptibility for each NA strain calculated using geometric mean titer (GMT). Since lower GMT corresponds to higher susceptibility, we use an inverse scale to show the relative susceptibility. The bars indicate 95% CIs obtained from bootstrapping. The lower rank (rank 1) indicates significantly higher susceptibility.

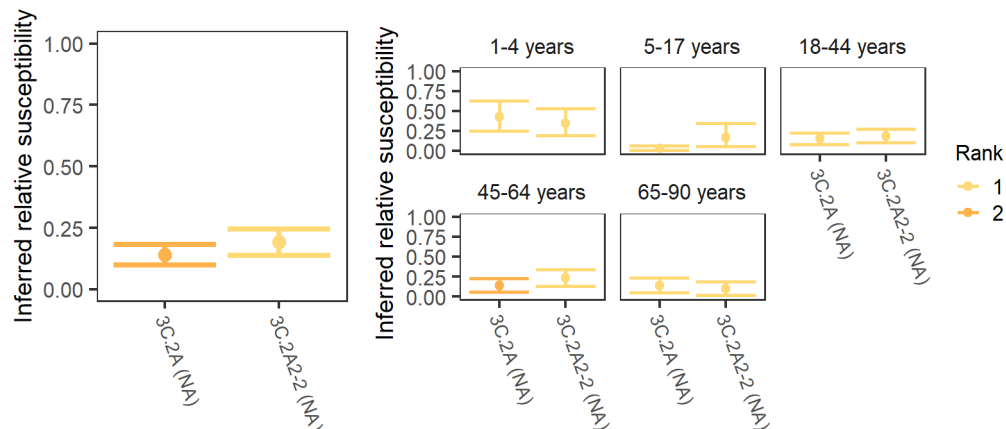


Fig S9. The inferred relative susceptibility and its rank to each NA reference strain using a 1:20 threshold. Inferred relative susceptibility and its rank to each reference strain for the whole population (left) and by age group (right). The bars indicate 95% CIs obtained from bootstrapping. The lower rank (rank 1) indicates significantly higher susceptibility.

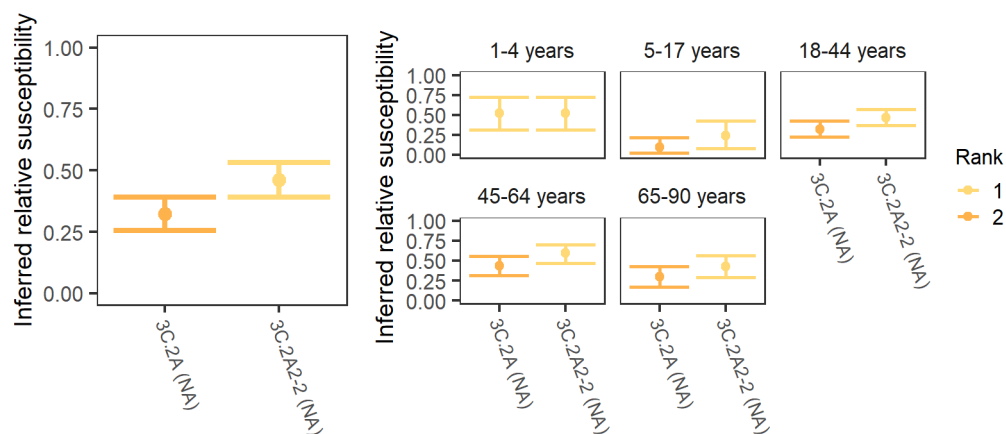


Fig S10. The inferred relative susceptibility and its rank to each NA reference strain using a 1:40 titer threshold. Inferred relative susceptibility and its rank to each reference strain for the whole population (left) and by age group (right). The bars indicate 95% CIs obtained from bootstrapping. The lower rank (rank 1) indicates significantly higher susceptibility.

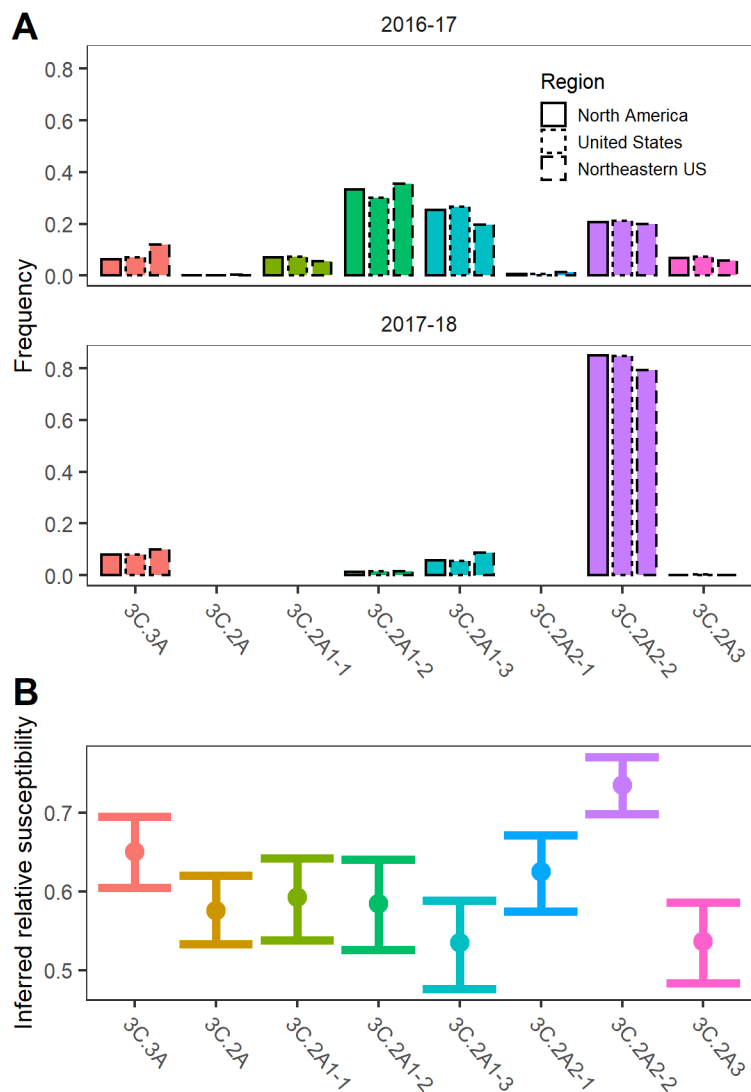


Fig S11. Comparison of H3 frequencies by clade (reference strain) and inferred relative susceptibilities. A. Frequencies of H3 sequences assigned to each test virus were calculated using GISAID sequences from North America, US, and the Northeastern US during the 2016-17 and 2017-18 season. B. Inferred relative susceptibilities to test viruses.

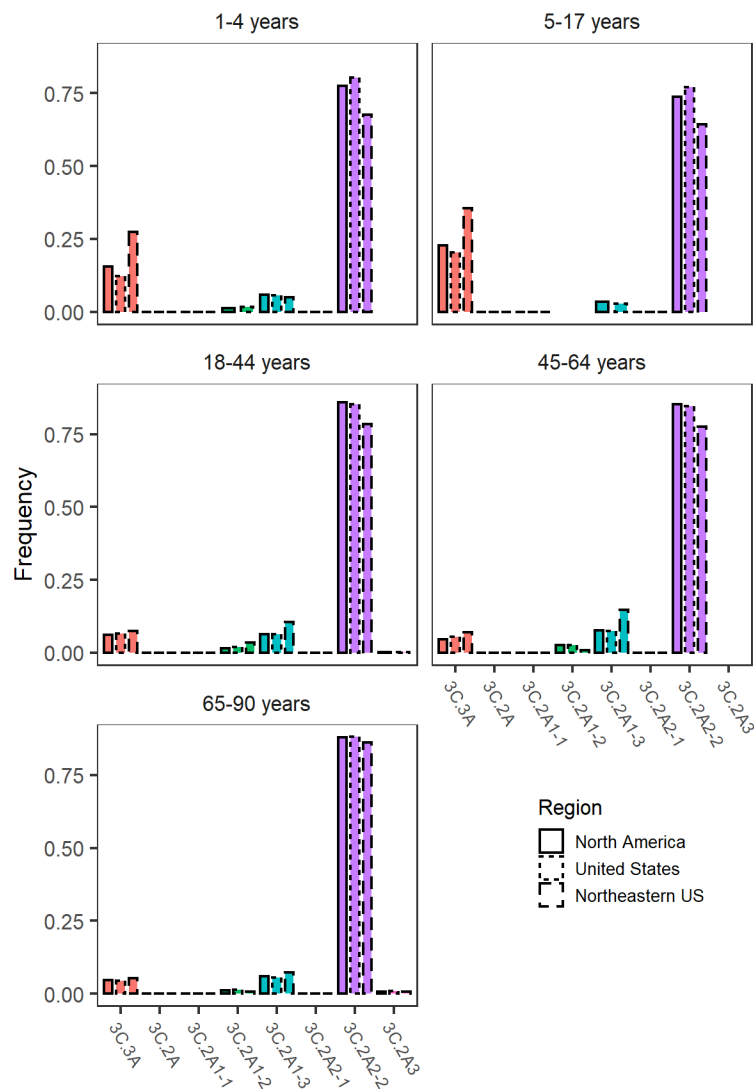


Fig S12. Frequencies of H3 sequences in the 2017-18 season assigned to each reference virus by age group. Frequencies were calculated using GISAID sequences collected in North America, US, and the Northeastern US, respectively.

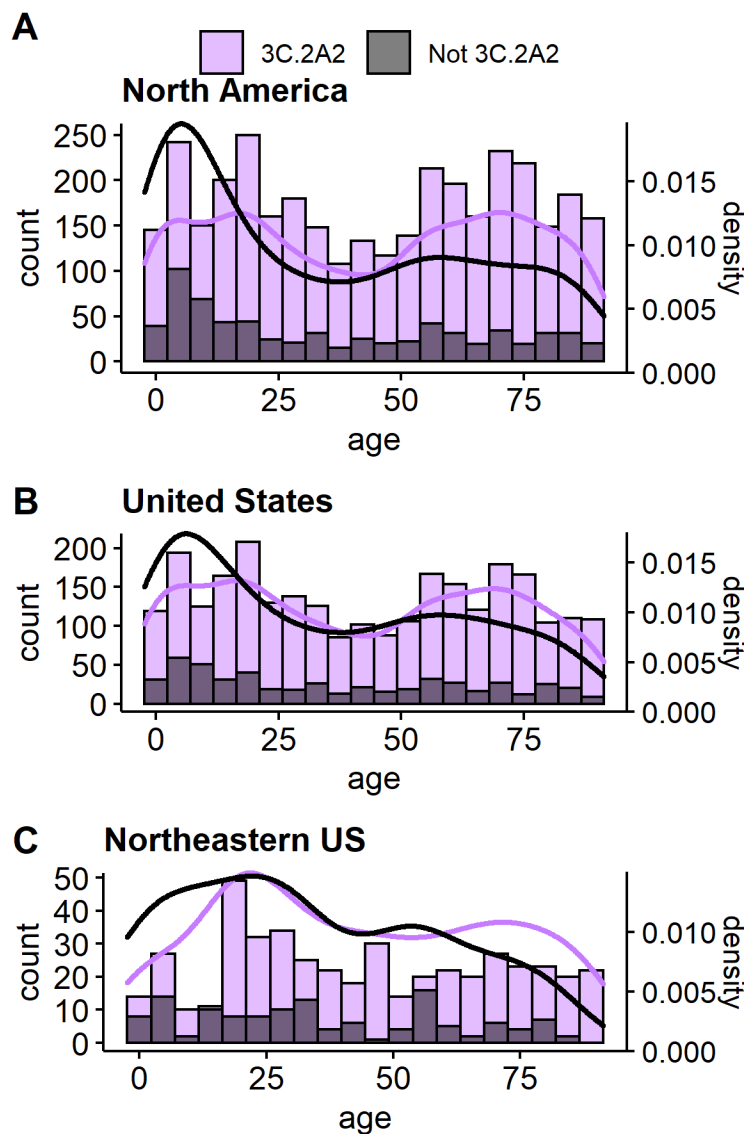


Fig S13. Age distributions of 3C.2A2-2-associated and other reference strains in the 2017-18 season. Strains from GISAID were characterized as belonging to the 3C.2A2 clade or not. Lines show the respective densities.

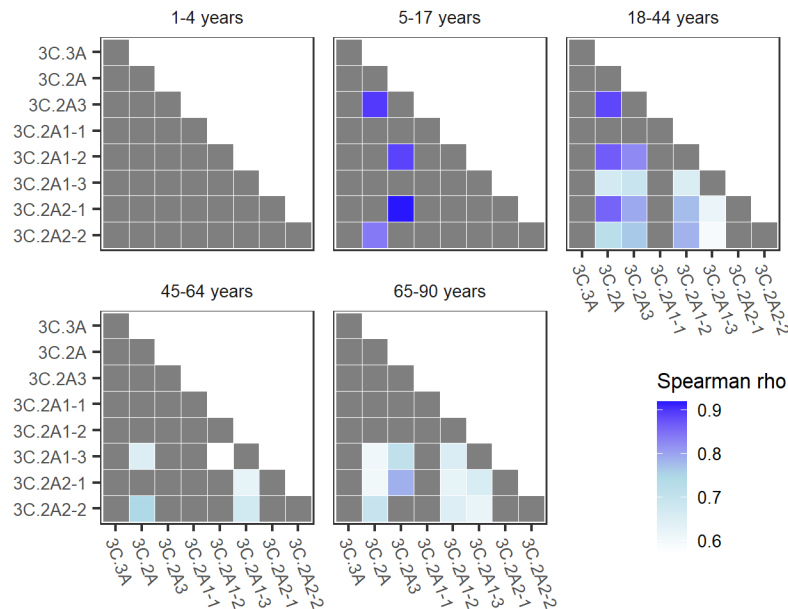


Fig S14. Compared to the youngest age group, older children and adults have significantly more weakly correlated titers to different strains. For each pair of viruses, the correlation between HA titers was calculated. The cells are colored blue if the correlation is significantly weaker in the age group compared to the same pair in 1- to 4-year-olds. Individuals with undetectable titers have been removed.

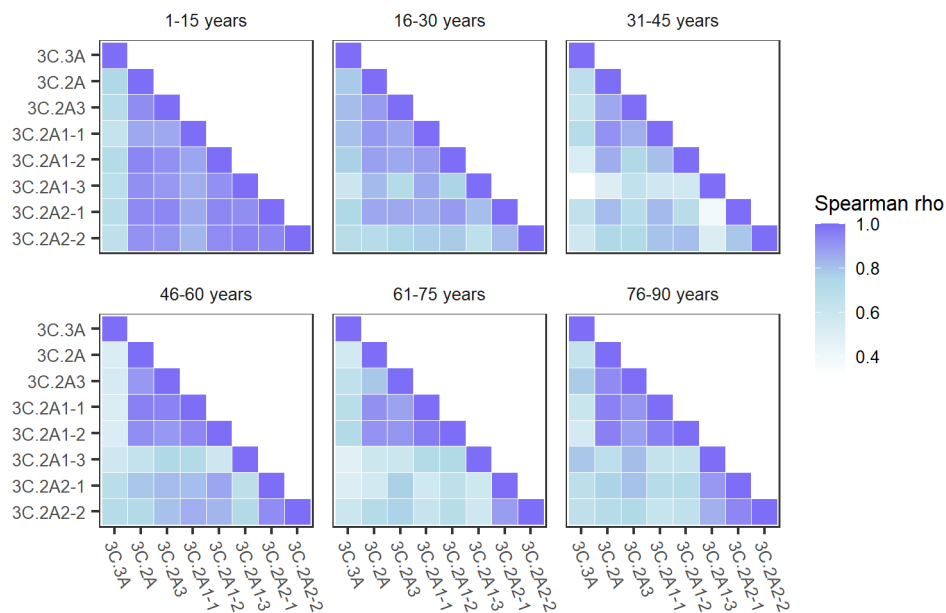


Fig S15. Correlations between titers to different test viruses by age group with equal number of years. For each pair of viruses, the correlation between HA titers was calculated. Individuals with undetectable titers have been removed.

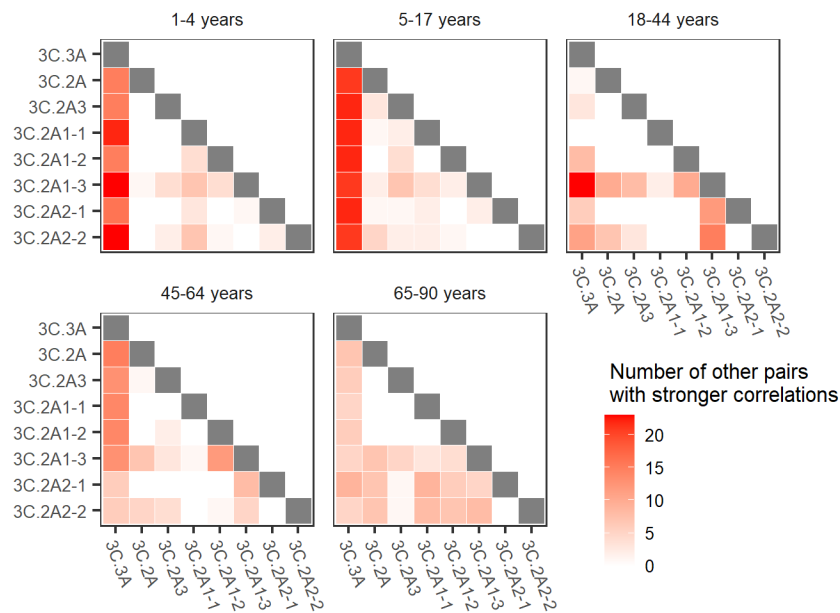


Fig S16. Weakly correlated reference pairs by age group. For each pair of reference viruses, the correlation between HA titers was calculated. The correlation coefficients of the virus pairs within each age group were compared to each other to test whether one correlation was significantly weaker than the other. Then, for each virus pair, the number of comparisons in which the pair's correlation was significantly weaker than that of other pairs (within that age group) was counted. Stronger colors indicate virus pairs with especially weak correlations.

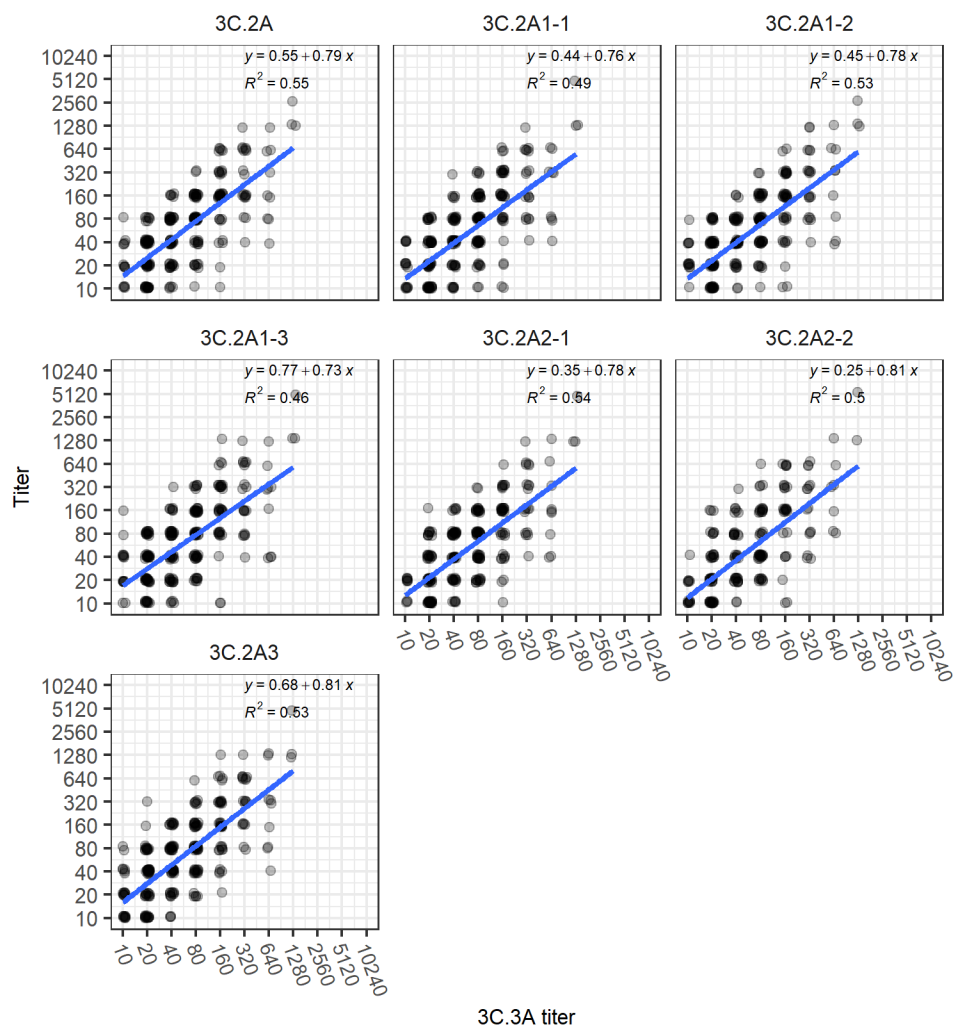


Fig S17. Correlations between 3C.3A titers and other titers in all ages. Points are slightly jittered. Blue line indicates the regression line. Individuals with undetectable titers to all strains were removed from the analysis.

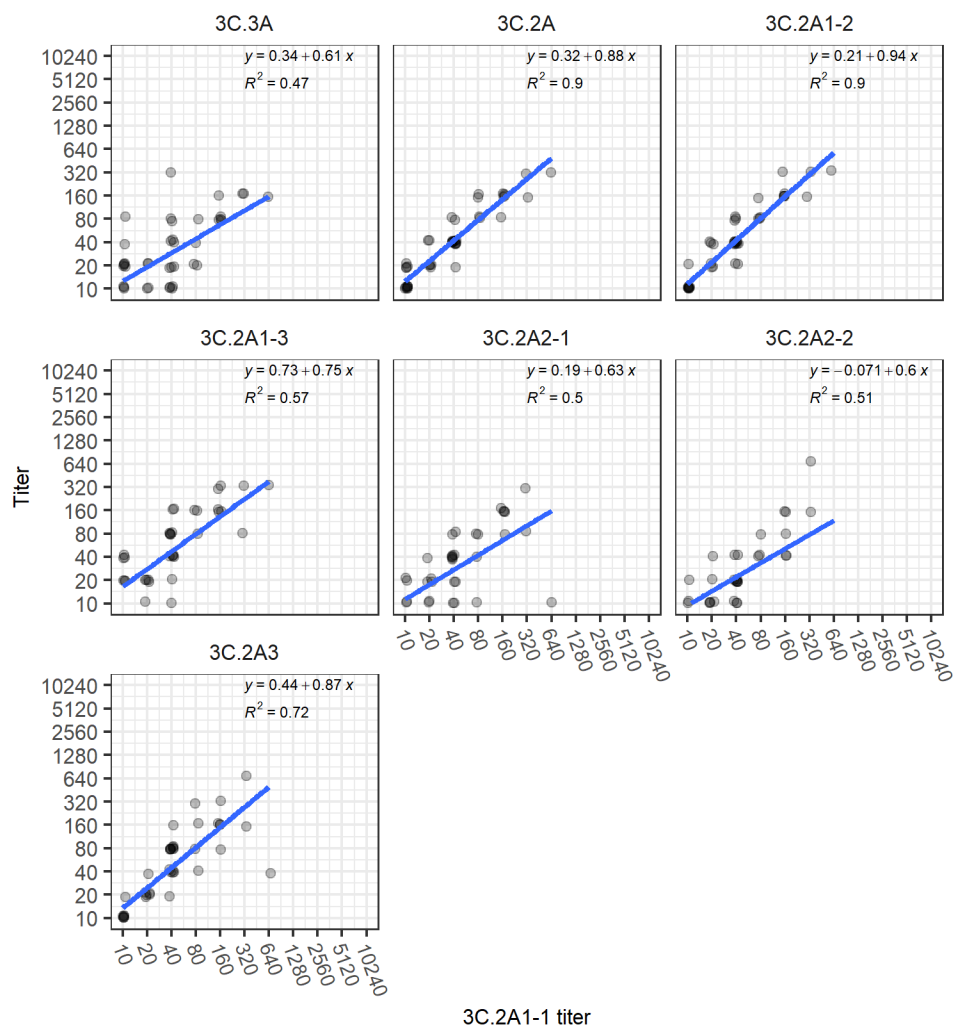


Fig S18. Correlation between 3C.2A1-1 titers and other titers in 45- to 90-year-olds. Points are slightly jittered. Blue line indicates the regression line. Individuals with undetectable titers to all strains were removed from the analysis.

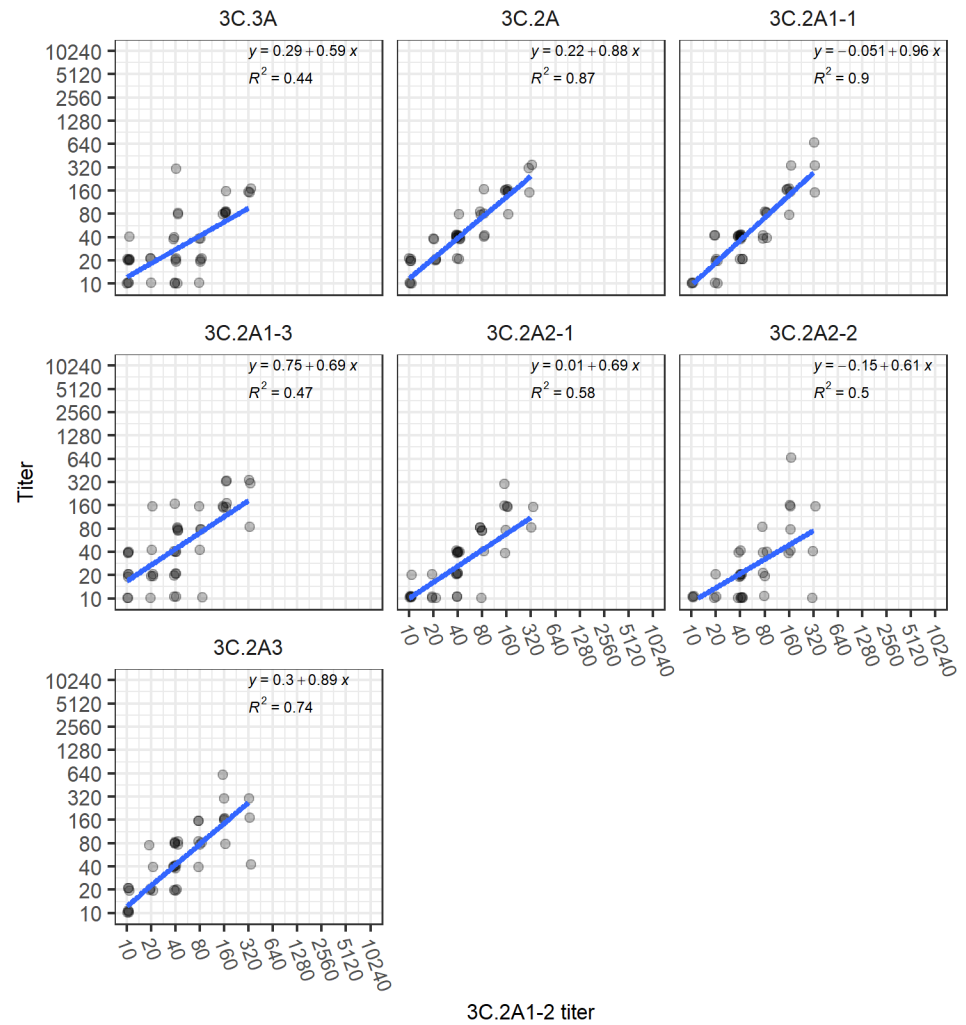


Fig S19. Correlations between 3C.2A1-2 titers and other titers in 45- to 90-year-olds. Points are slightly jittered. Blue line indicates the regression line. Individuals with undetectable titers to all strains were removed from the analysis.

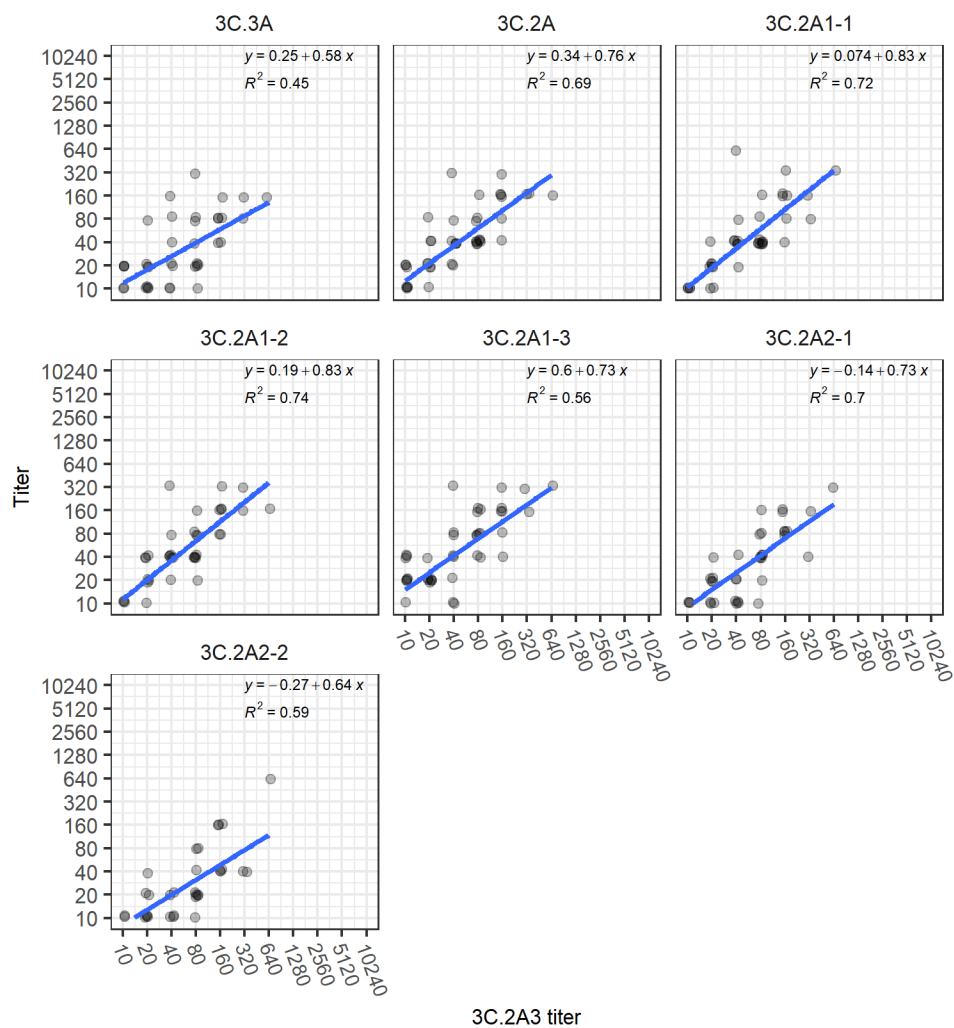


Fig S20. Correlations between 3C.2A3 titers and other titers in 45- to 90-year-olds. Points are slightly jittered. Blue line indicates the regression line. Individuals with undetectable titers to all strains were removed from the analysis.

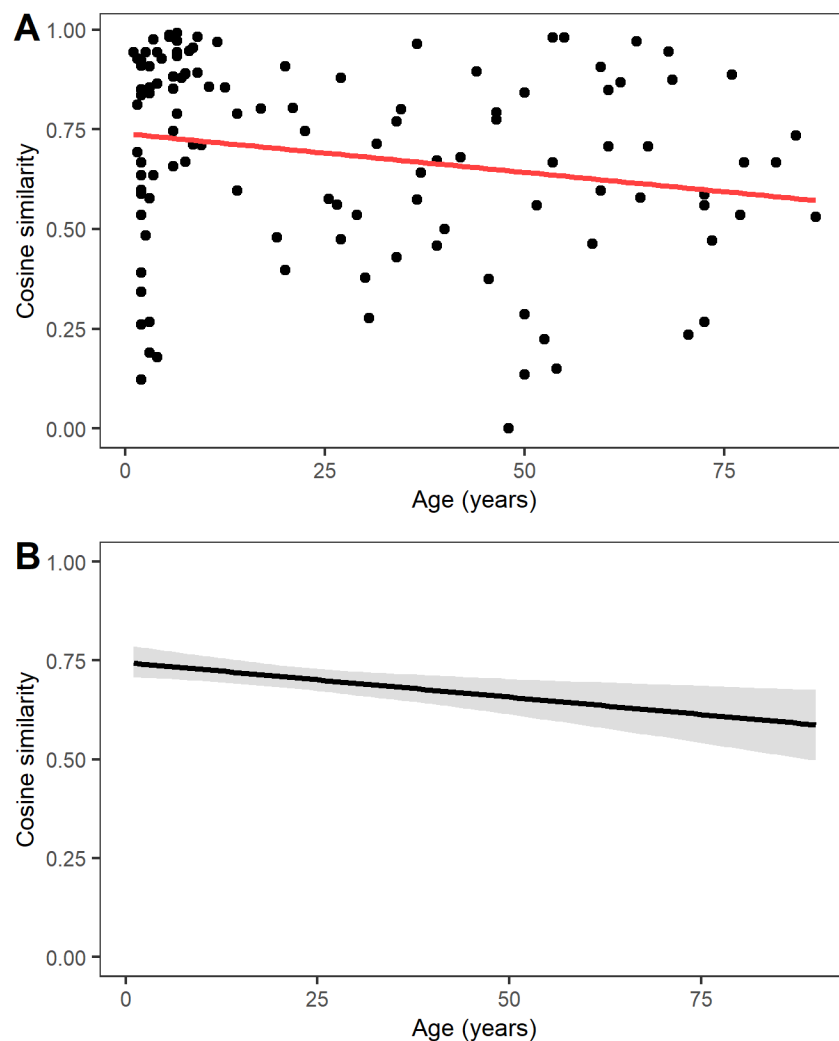


Fig S21. The similarity of HA-NA titer vectors declines with age. A. Cosine similarities of HA-NA titers between pairs of individuals (points) and the regression line (line). Each cosine similarity was calculated from a random pair of individuals within a 3-year age difference. B. The distribution of trends in cosine similarity by age obtained by regressing cosine similarity by age in 1000 different random pairings. The line indicates the mean of the 1000 regression lines, and the shade indicates the 95% interval of the regression lines.

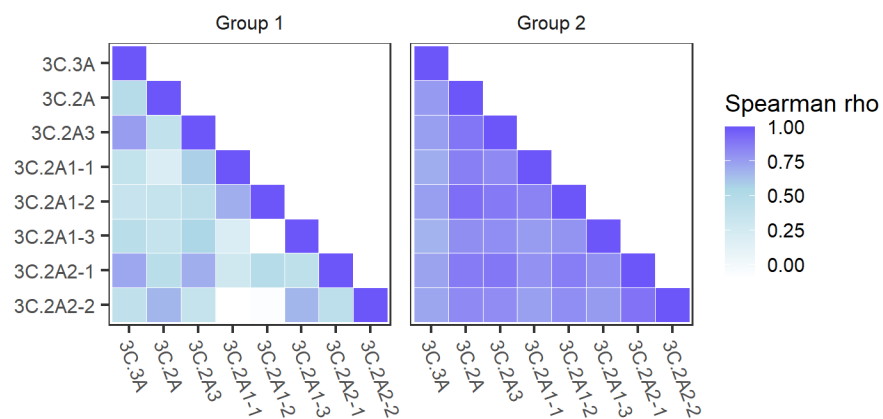


Fig S22. Correlations between titers to different strains within each group. Each cell is colored by the correlation coefficient. Individuals with undetectable titers to all reference viruses have been removed.

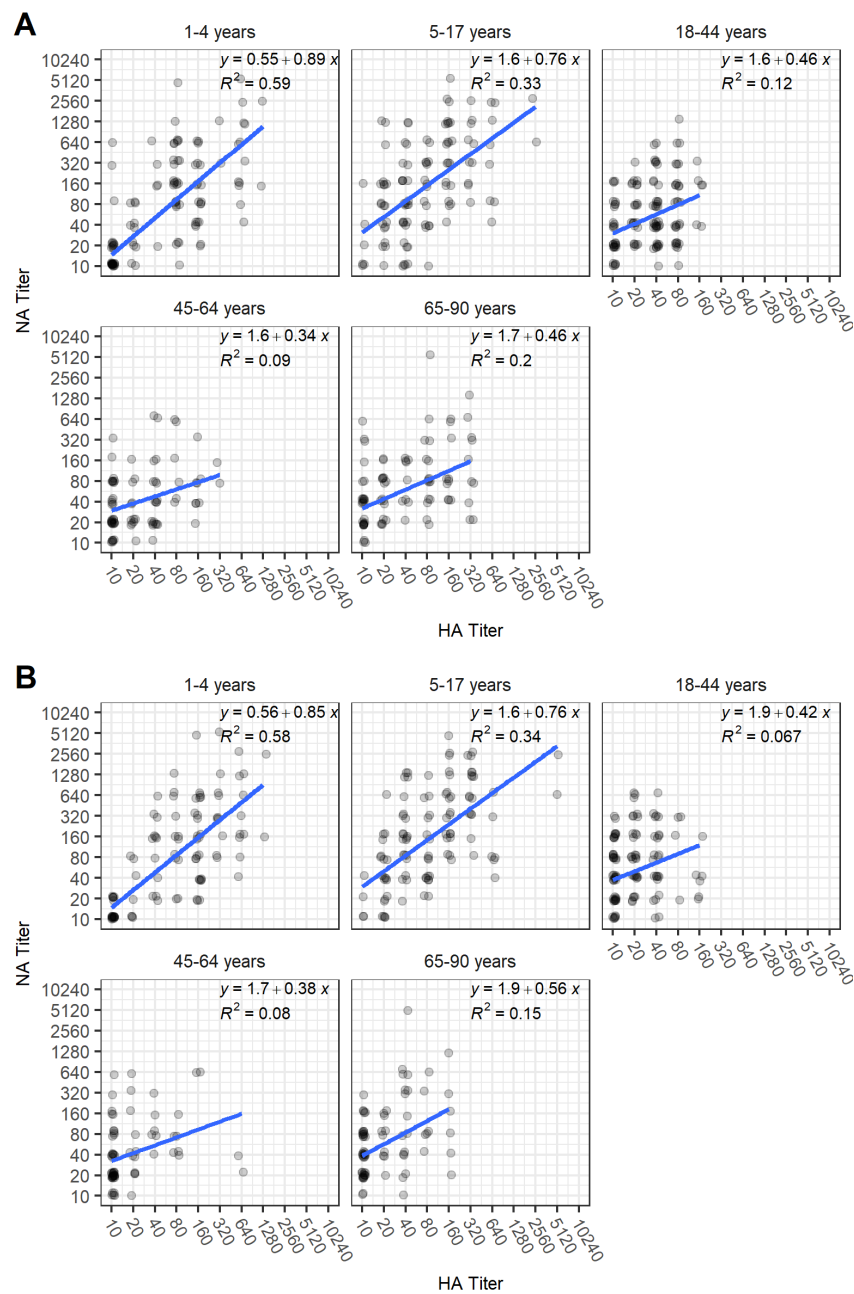


Fig S23. Correlations between HA and NA titers A. Titers to 3C.2A HA and NA. B. Titers to 3C.2A2 HA and NA. Points have been slightly jittered to show density. Blue lines indicate the regression lines.

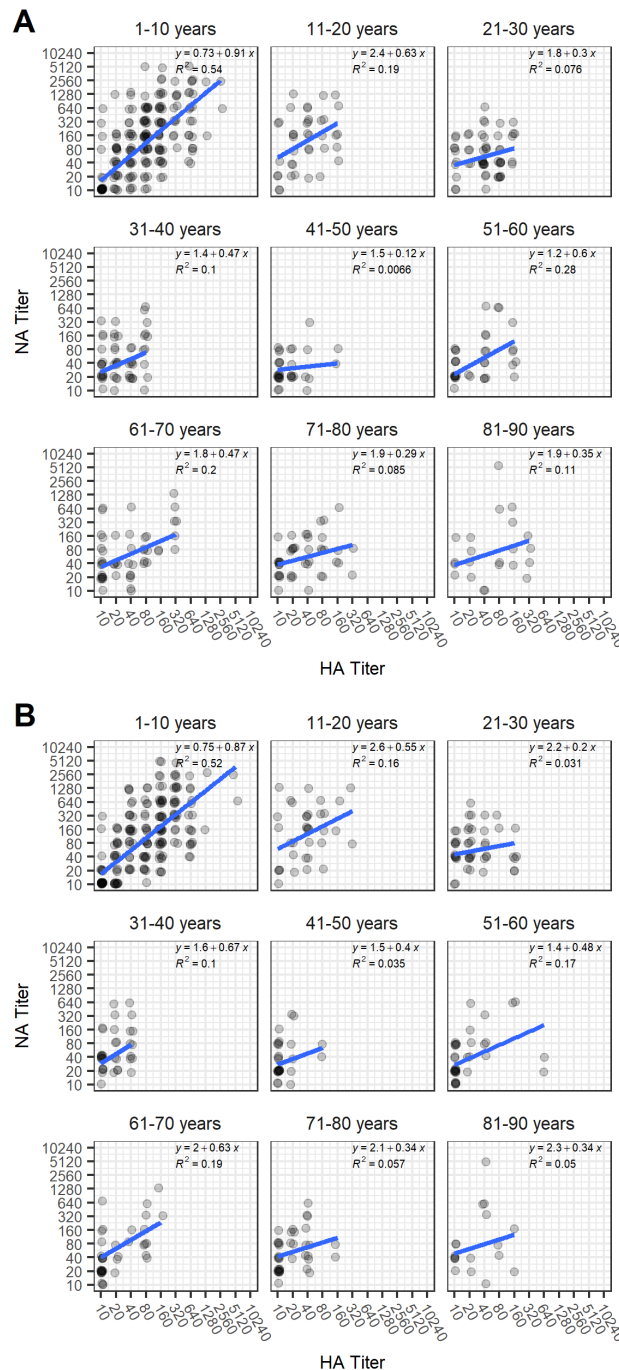


Fig S24. Correlations between HA and NA titers by 10-year age bins
 A. Titers to 3C.2A HA and NA. B. Titers to 3C.2A2 HA and NA. Points have been slightly jittered to show density. Blue lines indicate the regression lines.